Magazine of Concrete Research, 2007, **59**, No. 10, December, 757–769
doi: 10.1680/macr.2007.59.10.757

Tie-confined fibre-reinforced high-strength concrete short columns

U. K. Sharma*, P. Bhargava,† and S. A. Sheikh‡

National Institute of Technology; Indian Institute of Technology; University of Toronto

An experimental study was carried out to investigate the behaviour of steel fibre-reinforced high-strength concrete (HSC) short columns confined by square ties under monotonically increasing concentric compression. A total of 72 confined and 24 unconfined specimens were tested in this test programme. The test variables included aspect ratio and volume fraction of crimped steel fibres, volumetric ratio, yield strength and configuration of transverse tie reinforcement and concrete strength. The effects of these variables on the uniaxial behaviour of HSC short columns are presented and discussed. The results indicate that the addition of fibres to the HSC mix prevented the early spalling of the cover and increased the load-carrying capacity and ductility of the specimens over that of comparable non-fibre columns. The effect of mixed aspect ratio of fibres on the stress–strain behaviour of confined HSC was also studied by blending the short and long fibres. It is shown that a higher gain in column strength can be affected by the addition of shorter fibres, and longer fibres can provide better enhancements in the post-peak deformability.

Notation

A_g gross area of column cross-section
A_{st} sectional area of longitudinal reinforcement
E_c tangent modulus of elasticity of concrete
E_s modulus of elasticity of steel
f_c any general stress in confined stress–strain curve
f'_c cylinder compressive strength of concrete
f_{cc} peak stress of confined concrete
f_{co} unconfined strength of concrete column
f_{hcc} stress in tie at peak stress of confined concrete
f_y yield strength of longitudinal steel
f_{yh} yield strength of tie steel
l_f length of fibre
P'_c concrete load corresponding to first peak
P_{cc} peak-confined concrete load (corresponding to second peak)
P_{max} maximum applied load on the column
P_o theoretical capacity of column $= 0{\cdot}85 f'_c(A_g - A_{st}) + f_y A_{st}$
s spacing of ties
v_f volume fraction of fibres
ε' axial strain corresponding to the first peak, P'_c
ε_{cc} axial strain at peak-confined load, P_{cc}
ε_{c50c} axial strain at which the stress drops to 50% of peak in confined concrete
ε_{co} strain at peak load of unconfined concrete column
ε_{c50o} axial strain at which the stress drops to 50% of peak in unconfined concrete
ε'_h strain in tie at P'_c
ε_{hcc} strain in tie at P_{cc}
ε'_l strain in longitudinal steel at P'_c
ε_{lcc} strain in longitudinal steel at P_{cc}
ε_y yield strain of longitudinal reinforcement
ε_{yh} yield strain of tie reinforcement
ρ_l volumetric ratio of longitudinal steel
ρ_s volumetric ratio of ties

* Department of Civil Engineering, National Institute of Technology, Hamirpur—177 005, India
† Department of Civil Engineering, Indian Institute of Technology, Roorkee—247 667, India
‡ Civil Engineering Department, University of Toronto, Toronto, Canada M5S 1A4

(MCR 600002) Received 31 October 2006; last revised 1 June 2007; accepted 12 June 2007

Introduction

The gradual development of concrete technology has promoted the use of high-strength concrete (HSC) in reinforced concrete columns of multi-storey buildings owing to its wide range of advantages over normal-strength concrete. However, the advantages of using

HSC are offset by its poor post-peak behaviour. The studies undertaken in the past to investigate the confinement of HSC columns show that there is a consistent decrease in strength and deformability gains with increasing concrete strength.[1–4] These studies have indicated that a higher degree of confinement is required in columns with higher concrete strength than in columns with lower concrete strength to achieve similar advantages. HSC columns under the application of concentric loads suffer from yet another problem: premature cover spalling. Previous experimental and theoretical research has shown that the axial strength of HSC columns is affected by the early spalling of the cover and it can even result in lower column strength than theoretical squash load if sufficient confinement is not provided.[2,5,6]

The concept of using a combination of suitable randomly distributed discrete fibres with nominal amount of lateral steel has been discussed in the literature to ease the need for a high amount of confinement in the plastic hinge regions of HSC columns.[7–9] It has been shown that the use of fibres in the concrete mix provides indirect confinement to the concrete and improves the strength and ductility of columns. A review of literature, however, shows that the performance of HSC columns under the combined confining actions of transverse steel and discrete fibres has not been fully explored. The current paper reports the results of 72 tied-confined HSC short-column specimens cast with and without steel fibres and tested under concentric compression. The test variables included: fibre volume fraction; aspect ratio of fibres; parameters of confinement such as volumetric ratio; spacing and yield strength of ties; longitudinal reinforcement distribution and resulting tie configuration; and concrete compressive strength. The effect of blending short and long fibres (mixed aspect ratio) into the HSC mix has also been investigated.

Research significance

The addition of steel fibres is a promising and economical method to compensate for the loss in the post-peak deformability of HSC columns. However, research in this field is not conclusive. Earlier studies were either carried out mostly on spiral or tied-confined fibre-reinforced concrete small-scale cylinders or prisms without longitudinal steel[7,8,10] or the behaviour of tied-confined fibre-reinforced columns using normal-strength concrete was investigated.[11–13] Foster and Attard[9] reported the test results of concentrically and eccentrically loaded steel fibre-reinforced tied HSC columns. However, the effect of various parameters of fibres and transverse steel confinement on the peak and post-peak behaviour of confined concrete columns was not fully investigated. Most of the earlier studies mentioned that the cover spalling in HSC columns is either prevented or delayed by the addition of fibres. However, this important phenomenon has not been appropriately addressed in confined fibre-reinforced concrete columns. It may be emphasised here that the behaviour of cover concrete and hence the occurrence of spalling need to be tracked carefully to compute the contribution of confined concrete. The present paper addresses these issues through a comprehensive experimental research programme that involved testing of 96 specimens under concentric load.

Experimental programme

Test specimens

A total of 96 short HSC prism specimens were tested under monotonic concentric compression. They included 72 tie-confined specimens (150 mm × 150 mm × 600 mm) and 24 unconfined specimens. Unconfined specimens were of the same size as that of confined column specimens to establish the properties of unconfined plain and fibre-reinforced concrete and also to obtain a comparison of in-place prism strength of concrete with standard cylinder compressive strength. The details of the confined specimens are illustrated in Table 1 and Fig. 1. Table 2 gives the properties of unconfined specimens. The specimens were cast and tested in duplicate in order to obtain the average of two results, thus making 36 confined and 12 unconfined independent column designs. Each reported result is therefore the average of two test units. The crimped steel fibres were used with three volume fractions (1·0%, 1·5% and 2·0%) and two aspect ratios (20 and 40). For each tie configuration, the column specimens were cast without fibres and with fibres of two different aspect ratios. A few specimens were also cast by blending the short and long fibres in equal weight at total volume fraction of 1·5% to assess the effect of mixed aspect ratio. Concrete cover of 10 mm was provided in all the confined specimens.

Failure of the specimens was forced in the test region, which was equal to 300 mm in the middle of the specimen height, by reducing the spacing of the lateral reinforcement outside the test region to half of the specified spacing in the test region. The specimens were also externally confined in the end regions by 10 mm thick steel collars to prevent further premature end failure. The specimens were cast in steel moulds in the laboratory. The standard (100 × 200 mm) cylinders (108 in number) were also cast with the prism specimens. After 24 hours, the specimens were removed from the moulds and submerged in a water tank for curing. The water curing lasted for 28 days, after which the specimens were left in the laboratory at ambient temperature until the time of testing. The testing commenced 90 days after casting.

Table 1. Properties of confined specimens

Specimens	f'_c: MPa	Longitudinal steel*		Lateral ties†					Fibres	
		ρ_l: %	f_y: MPa	Dia.: mm	Arrangement	s: mm	ρ_s: %	f_{yh}: MPa	v_f: %	Aspect ratio: l_f/d
SA1	62·20	2·01	395	8	A	50	3·3	412	—	—
SA2									1·5	20
SA3									1·5	20 (50%) + 40 (50%)
SA4									1·5	40
SB1	62·80	2·01	395	8	A	75	2·2	412	—	—
SB2									1·5	20
SB3									1·5	40
SC1	61·85	2·01	395	8	A	50	3·3	520	—	—
SC2									1·5	20
SC3									1·5	20 (50%) + 40 (50%)
SC4									1·5	40
SD1	63·35	4·02	395	8	B	50	5·6	412	—	—
SD2									1·5	20
SD3									1·5	40
SE1	82·50	2·01	395	8	A	30	5·5	412	—	—
SE2									1·5	20
SE3									1·5	40
SF1	81·75	2·01	395	8	A	50	3·3	412	—	—
SF2									1·5	20
SF3									1·5	20 (50%) + 40 (50%)
SF4									1·5	40
SF5									1·0	20
SF6									1·0	40
SF7									2·0	20
SG1	83·15	2·01	395	8	A	75	2·2	412	—	—
SG2									1·5	20
SG3									1·5	40
SH1	81·80	2·01	395	8	A	50	3·3	520	—	—
SH2									1·5	20
SH3									1·5	40
SI1	82·55	4·02	395	8	B	50	5·6	412	—	—
SI2									1·5	20
SI3									1·5	20 (50%) + 40 (50%)
SI4									1·5	40
SI5									1·0	20
SI6									1·0	40

*$\varepsilon_y = 0{\cdot}0023$ for $f_y = 395$ MPa , †$\varepsilon_{yh} = 0{\cdot}0024$ for $f_{yh} = 412$ MPa and $\varepsilon_{yh} = 0{\cdot}0026$ for $f_{yh} = 520$ MPa

Material properties

The concrete was made with ordinary Portland cement, natural river sand, crushed limestone aggregate of maximum size 10 mm, tap water, silica fume and superplasticiser. The concrete mixes of two different specified compressive strengths were employed (Table 1). The fibres used were flat crimped steel fibres with a cross-section of 2 mm × 0·6 mm (equivalent diameter = 1·24 mm). They were of two different lengths, short (25 mm) and long (50 mm), to give nominal aspect ratios of 20 and 40 respectively. The longitudinal reinforcement consisted of 12 mm diameter deformed bars of 395 MPa yield strength, and two different grades (412 MPa and 520 MPa) of reinforcing steel with a diameter of 8 mm were used as lateral tie reinforcement. The average stress–strain relationships, established by performing at least three coupon tests for each type of reinforcement bar, are illustrated in Fig. 2. The standard plain concrete cylinders were tested to determine the nominal strength of concrete on the day of testing of column specimens.

Instrumentation and testing procedure

The strains in the longitudinal and lateral steel were measured with electrical resistance strain gauges. The strain gauges were installed on the two opposite longitudinal steel bars at their middle lengths. Similarly, two gauges were glued at two locations on the ties at approximately mid-length of the specimen as shown in Fig. 1. The axial displacement of the specimens was recorded using four linear variable differential transducers (LVDTs). Two LVDTs were attached on the opposite faces with the help of steel clamps to give a gauge length of 250 mm. Two LVDTs were mounted on the other two faces of the specimen attached to the end steel collars. In case the steel clamps became dislodged owing to a sudden specimen failure or to concrete

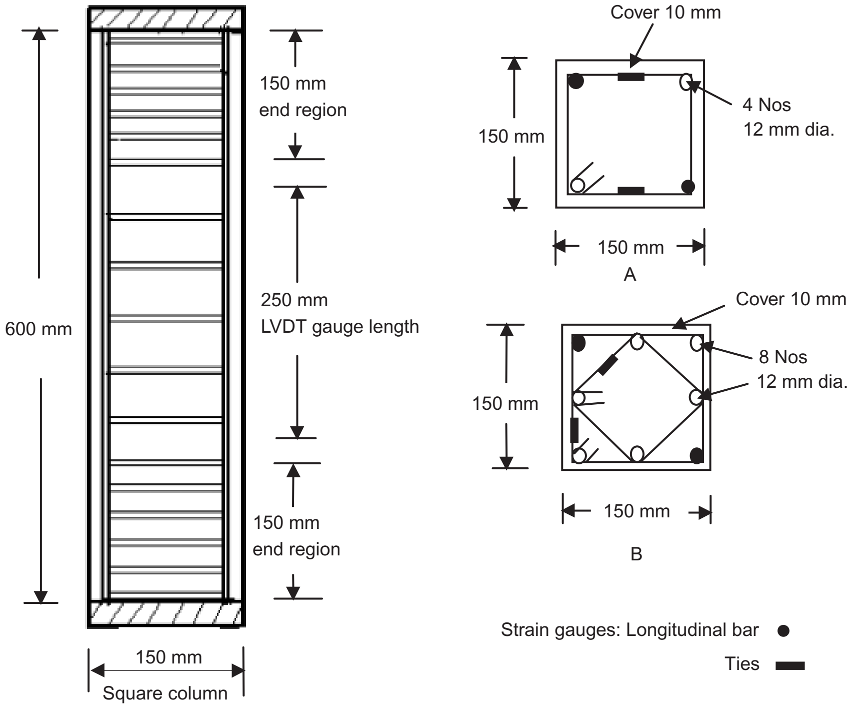

Fig. 1. Details of column specimens, reinforcement arrangement and location of strain gauges

Table 2. Properties and results of unconfined specimens

Specimens	f'_c: MPa	Fibres		f_{co}: MPa	ε_{co}	ε_{c50o}	E_c: MPa	A_{cuo}: MPa
		v_f: %	l_f/d					
LP	61·90	1·5	—	54·47	0·0023	*	31645	0·179
LF1		1·5	20	62·87	0·0036	0·012	32215	0·615
LF2		1·5	20 (50%) + 40 (50%)	59·58	0·0039	0·017	31720	0·812
LF3			40	57·80	0·0041	0·021	31154	0·936
UP	82·25	1·5	—	74·20	0·0025	*	34465	0·185
UF1		1·5	20	80·55	0·0034	0·0065	35265	0·400
UF2		1·5	20 (50%) + 40 (50%)	78·17	0·0038	0·0092	35120	0·487
UF3		1·0	40	75·99	0·0042	0·0130	34425	0·703
UF4		1·0	20	78·53	0·0033	0·0058	34655	0·378
UF5		2·0	40	74·04	0·0037	0·0080	33410	0·452
UF6		2·0	20	85·50	0·0042	0·0110	35840	0·667
UF7			40	77·71	0·0046	0·0190	34080	1·016

* Could not be measured

spalling, the LVDTS mounted on the end collars provided a reliable source of measurements at large strains. LVDTs had a displacement range of 50 mm. Loads were recorded through a 3000 kN capacity load cell. The recorded data from the LVDTs, strain gauges and load cell were fed into a data acquisition system and stored on a computer.

The top and bottom ends of the specimens were slightly ground to remove surface unevenness and protruding fibres. The test specimens were loaded using a 5000 kN capacity hydraulic universal testing machine with load-controlled capabilities. The monotonic concentric compression was applied at a slow rate (0·05 MPa/s) to capture the post-peak part of the measured load–deformation curves by manually controlling the oil pressure. The loading was continued until failure, which was determined primarily by rupture of the lateral reinforcement together with buckling of the longitudinal bars.

Test results

The test results are given in Table 2 for unconfined specimens and in Tables 3 and 4 for confined column specimens. The unconfined plain concrete specimens had a sudden explosive type of failure at the maximum axial load. The complete load–deflection curves for

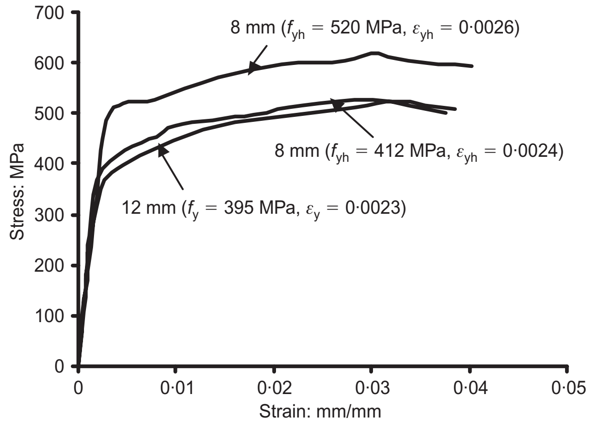

Fig. 2. Stress–strain curves for reinforcing bars

these specimens could not be obtained with the present testing facility, and no readings could be taken after their brittle failure. However, the load–deflection curves of unconfined fibre concrete specimens could be recorded to a reasonable extent beyond peak load. The recorded average axial stress–strain curves of unconfined concrete specimens are given in Fig. 3. It was observed that the strength of unconfined plain concrete prism specimens was considerably lower than the strength measured from standard cylinders. The average prism strength was measured as 88% and 90% of the average cylinder strength for the lower and upper HSCs, respectively. However, the commonly used ratio of 0·85 was still used for evaluating the theoretical concrete section capacity of the specimens tested in the present study.

The response curves of confined columns between applied axial load, P, and the average axial strain measured by the LVDTs are given in Fig. 4. Each curve represents the average of twin specimens. To facilitate the comparison of behaviour of different columns, the ordinates in the curves have been non-dimensionalised with respect to the theoretical capacity of columns, P_o.

Table 3. Results of confined specimens

Specimen	P_{max}: kN	P_{max}/P_o	P'_c: kN	P'_c/P_{oc}	P_{cc}: kN	P_{cc}/P_{occ}	At P'_c		At P_{cc}	
							ε'_l: $\mu\varepsilon$	ε'_h: $\mu\varepsilon$	ε_{lcc}: $\mu\varepsilon$	ε_{hcc}: $\mu\varepsilon$
SA1	1334	0·992	1155	0·990	985	1·291	2849	1141	4879	2356
SA2	1547	1·151	1368	1·173	1076	1·410	3878	542	11479	2897
SA3	1532	1·139	1353	1·160	1053	1·380	4015	678	21458	2475
SA4	1468	1·092	1289	1·105	1030	1·350	3887	778	26874	2297
SB1	1364	1·005	1185	1·006	917	1·189	2142	*	*	*
SB2	1478	1·090	1299	1·100	960	1·245	3672	680	6448	*
SB3	1419	1·046	1240	1·053	1010	1·310	5450	1040	8490	1640
SC1	1308	0·977	1133	0·977	1042	1·372	2448	1155	4678	2150
SC2	1555	1·162	1376	1·187	1095	1·443	3145	*	14220	2965
SC3	1477	1·104	1298	1·119	1032	1·359	4150	1260	15040	*
SC4	1485	1·109	1306	1·127	1031	1·358	3995	880	14780	2620
SD1	1626	1·069	1171	1·007	1268	1·683	2634	1425	7465	3224
SD2	1735	1·141	1377	1·184	1340	1·779	3426	643	7122	3567
SD3	1623	1·067	1265	1·087	1198	1·590	4139	1146	29874	4257
SE1	1641	0·951	1463	0·946	1400	1·382	2346	1247	4931	2775
SE2	1707	0·989	1529	0·989	1466	1·448	3456	743	11472	2948
SE3	1654	0·968	1475	0·964	1400	1·382	3789	1143	8567	3547
SF1	1604	0·937	1433	0·935	1220	1·216	2347	1150	4420	1964
SF2	1812	1·059	1633	1·065	1288	1·284	3846	457	5013	1447
SF3	1840	1·075	1661	1·084	1314	1·310	3497	1034	6730	2163
SF4	1745	1·019	1566	1·022	1244	1·240	4567	1083	12367	2021
SF5	1722	1·010	1544	1·010	1248	1·244	3142	1185	4870	*
SF6	1774	1·037	1595	1·041	1264	1·260	2789	965	4760	1745
SF7	1897	1·109	1719	1·122	1374	1·370	4586	685	9435	2280
SG1	1730	0·995	1551	0·995	1125	1·100	2481	1362	*	*
SG2	1880	1·082	1701	1·091	1183	1·159	2750	745	4010	*
SG3	1834	1·056	1655	1·062	1143	1·120	4140	1080	5860	1440
SH1	1621	0·946	1446	0·943	1304	1·300	2740	*	4120	*
SH2	1858	1·085	1679	1·095	1402	1·397	2820	475	7870	1830
SH3	1757	1·026	1578	1·029	1310	1·306	4560	1065	10250	2280
SI1	1819	0·971	1461	0·964	1401	1·430	2635	1195	6715	2870
SI2	2097	1·119	1739	1·147	1578	1·608	3370	340	9590	2970
SI3	2103	1·123	1745	1·152	1482	1·510	4620	820	16210	3130
SI4	1992	1·063	1634	1·078	1456	1·485	3730	815	15200	3635
SI5	1946	1·038	1588	1·048	1468	1·496	2940	1220	9330	2150
SI6	1870	1·000	1500	0·990	1406	1·433	3485	1290	14670	2710

*Could not be measured

Table 4. Deformability of confined specimens

Specimen	ε'	$\varepsilon'/\varepsilon_{co}$	ε_{cc}	$\varepsilon_{cc}/\varepsilon_{co}$	ε_{c85c}	$\varepsilon_{c85c}/\varepsilon_{co}$	ε_{c50c}	$\varepsilon_{c50c}/\varepsilon_{co}$	A_{cuc}: MPa	A_{cuc}/A_{cuo}
SA1	0·0023	0·97	0·0038	1·63	0·0065	2·74	0·0110	4·64	0·791	4·42
SA2	0·0035	1·49	0·0121	5·10	0·0175	7·38	0·0297	12·53	1·732	9·67
SA3	0·0038	1·63	0·0146	6·16	0·0215	9·07	0·0400	16·87	2·206	12·32
SA4	0·0042	1·79	0·0156	6·58	0·0252	10·63	0·0460	19·41	2·465	13·77
SB1	0·0023	0·99	0·0031	1·32	0·0037	1·58	0·0055	2·32	0·236	1·32
SB2	0·0033	1·42	0·0056	2·39	0·0085	3·59	0·0135	5·69	0·792	4·42
SB3	0·0041	1·76	0·0077	3·27	0·012	5·06	0·0262	11·05	1·449	8·09
SC1	0·0022	0·94	0·0042	1·80	0·0068	2·87	0·0140	5·91	0·870	4·86
SC2	0·0033	1·43	0·0136	5·73	0·0205	8·65	0·0310	13·08	2·265	12·65
SC3	0·0039	1·67	0·0146	6·16	0·0258	10·89	0·0355	14·98	2·248	12·56
SC4	0·0038	1·63	0·0158	6·66	0·0305	12·87	0·0480	20·25	2·735	15·27
SD1	0·0026	1·11	0·0071	3·01	0·0140	5·91	0·0320	13·50	2·178	12·17
SD2	0·0038	1·63	0·0159	6·71	0·0285	12·02	0·0530	22·36	3·694	20·63
SD3	0·0044	1·88	0·0235	9·91	0·0430	18·14	0·0635	26·79	4·216	23·55
SE1	0·0022	0·87	0·0051	1·96	0·0081	3·11	0·0140	5·38	1·507	8·14
SE2	0·0029	1·15	0·0114	4·38	0·0180	6·92	0·0380	14·61	3·142	16·98
SE3	0·0033	1·29	0·0179	6·88	0·0320	12·30	0·0526	20·23	3·783	20·43
SF1	0·0022	0·85	0·0037	1·43	0·0048	1·84	0·0069	2·65	0·583	3·36
SF2	0·0033	1·28	0·0052	2·02	0·0076	2·95	0·0155	5·96	1·192	6·44
SF3	0·0036	1·41	0·0064	2·48	0·0096	3·69	0·0210	8·07	1·450	7·84
SF4	0·0041	1·61	0·0098	3·79	0·0139	5·34	0·0212	8·15	1·693	9·15
SF5	0·0035	1·36	0·0047	1·84	0·0062	2·38	0·0135	5·19	0·711	3·85
SF6	0·0035	1·35	0·0050	1·95	0·0068	2·62	0·0165	6·35	0·908	4·91
SF7	0·0041	1·60	0·0084	3·25	0·0155	5·96	0·0299	11·50	1·983	10·72
SG1	0·0025	0·96	0·0028	1·08	0·0035	1·35	0·0042	1·61	0·281	1·52
SG2	0·0031	1·19	0·0037	1·44	0·0044	1·69	0·0089	3·42	0·601	3·25
SG3	0·0038	1·49	0·0054	2·10	0·0079	3·04	0·0134	5·16	0·779	4·21
SH1	0·0023	0·89	0·0036	1·39	0·0061	2·34	0·0098	3·77	0·810	4·38
SH2	0·0036	1·41	0·0071	2·76	0·0098	3·77	0·0155	5·96	1·695	9·16
SH3	0·0040	1·56	0·0099	3·83	0·0145	5·58	0·0345	13·27	2·096	11·32
SI1	0·0025	0·97	0·0063	2·42	0·0116	4·46	0·0210	8·077	2·045	11·05
SI2	0·0035	1·36	0·0104	4·00	0·0212	8·15	0·0433	16·69	3·529	19·08
SI3	0·0039	1·53	0·0148	5·69	0·024	9·23	0·0510	19·61	4·301	23·25
SI4	0·0040	1·57	0·0167	6·42	0·0377	14·50	0·0569	21·89	4·309	23·29
SI5	0·0031	1·22	0·0087	3·38	0·0172	6·61	0·0277	10·65	2·632	14·23
SI6	0·0036	1·41	0·0121	4·65	0·0225	8·65	0·0371	14·27	3·256	17·60

Behaviour of concrete cover in confined specimens

The concrete cover in HSC columns separates abruptly with a loud noise and a sudden loss of the columns' load-carrying capacity.[2,5,6] In all the HSC columns of Cusson and Paultre,[2] cover separated at axial strain values of 0·0023 to 0·0033. Various theories have been put forward to explain early cover spalling in HSC columns.[5,14–16] Tie steel creates a separation between the core and the cover concrete that may result in early separation of the cover. If lateral steel contents are not high enough to provide the confinement to the core to compensate for this loss, the column capacity will be lower than the theoretical squash capacity. It has been reported that premature cover spalling in HSC columns containing an insufficient amount of confinement steel resulted in a column strength lower than the theoretical squash load. The test results of confined non-fibre HSC specimens of the present study also corroborate these earlier findings.

The cover spalling in confined fibre-reinforced column specimens tested in this programme was observed to be much delayed and quite gradual. Fine irregular surface cracks appeared either slightly before or at the peak of load–strain curves of these specimens. With the increase in applied axial strain, the number of cracks increased at a reduced rate compared with the confined non-fibre concrete columns. Slowly, these cracks widened with a decrease in applied load. The cracking of the cover gradually led to its spalling. The extent of cracking in the cover, rate of decrease of load after peak and axial strain at spalling depended upon the aspect ratio of fibres (100% short fibres or 100% long fibres or blended fibres), volume fraction of fibres, concrete strength and confinement level. For the same concrete strength and degree of tie confinement, the higher the aspect ratio and volume fraction of fibres, the slower was the rate of growth of cracks and the higher was the axial strain at spalling. Concrete spalling was more gradual and the axial strain at spalling was higher in the case of specimens with lower-

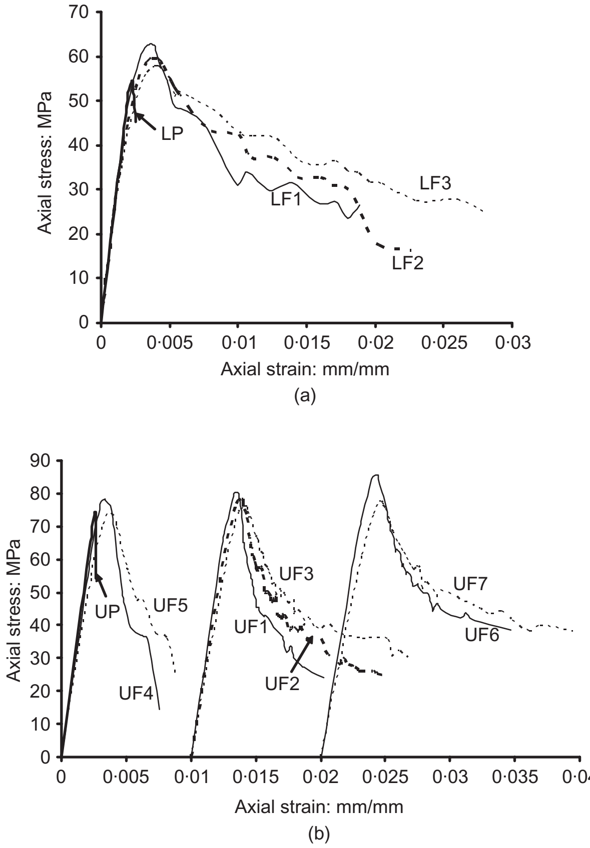

Fig. 3. (a) and (b) Axial stress–strain curves of unconfined plain and fibrous concrete specimens

strength concrete than in higher-strength concrete column specimens. The effect of degree of confinement was less marked on the occurrence of spalling. The spalling of cover could be clearly marked in most of the specimens, especially in columns having higher-strength concrete. Unlike in non-fibre HSC specimens, the cover did not fall off even when it had completely separated from the core. The axial column strain at which the cover spalled for any confined fibre-reinforced column was observed to be approximately close to the strain ε_{c50o} (axial strain at which the stress drops to 50% of peak in unconfined fibre-reinforced concrete). Therefore, at an axial strain value corresponding to ε_{c50o}, cover of confined column specimens can be assumed to have spalled off completely.

The delayed spalling in fibre-reinforced HSC column specimens can be attributed to the improved crack arresting mechanism and greater integrity of the material caused by the presence of fibres.

Behaviour of confined specimens

All fibre and non-fibre confined specimens were characterised sequentially by the development of surface cracks, yielding of longitudinal steel, cover spalling, yielding of lateral steel, fracture of spiral or ties, buckling of longitudinal bars and crushing of core concrete. All the specimens initially behaved in a similar manner and exhibited a relatively linear load–deformation response in the ascending part up to the peak, which is typical of HSC. Cracking and subsequent cover spalling often resulted in a sudden drop in load in confined non-fibre specimens and a gradual drop in load in confined fibre specimens. Post-spalling behaviour of non-fibre specimens depended solely upon their confinement levels. In the case of fibre-reinforced column specimens, in addition to the lateral steel, the properties of fibres such as aspect ratio and volume fraction determine the specimen behaviour. Load resistance of well-confined specimens again increased to a second peak, while poorly confined specimens showed a continuous decay in strength. The poorly confined non-fibre concrete specimens, especially columns with 75 mm spacing of ties, failed immediately after the first peak load was reached, indicating that the spacing of lateral steel was too large to provide effective confinement. However, the failure of these specimens in the presence of fibres was not that brittle.

Finally, the confined non-fibre specimens mostly failed by the fracture of ties followed by buckling of longitudinal steel, crushing of core or sometimes by the formation of inclined failure plane. The failure of fibre-reinforced specimens was marked by significant bulging of the specimen in the lateral direction with cracking, which gradually led to the fracture of ties and buckling of longitudinal steel. The bulging, which signals a ductile failure, was observed more in specimens with only longer fibres or with blended fibres compared with specimens with only short fibres. Also, the failure of fibre column specimens with a higher volume fraction of fibres was more gradual for the same aspect ratio of fibres, concrete strength and confinement level. Fig. 5 gives the appearance of a few specimens at the end of testing.

Confined concrete contribution curves

Behaviour of the confined concrete was determined following the procedure suggested by Sheikh and Uzumeri[17] and is explained in the following. The concrete contribution P_c at a certain deformation was determined by subtracting the contribution of longitudinal steel from the applied load P. The load carried by the longitudinal steel was determined from the stress–strain curves obtained from the tension test. The concrete contribution P_c was then non-dimensionalised with respect to gross concrete area force P_{oc} and core concrete area force P_{occ}, where $P_{oc} = 0.85 f'_c A_c$ and $P_{occ} = 0.85 f'_c A_{cc}$. Thus, the concrete contribution can be shown by two curves P_c/P_{oc} and P_c/P_{occ} and the behaviour of confined concrete shall be the combination of these two computed curves (Fig. 6). As the cover in these HSC specimens remained intact until the first peak was reached in both non-fibre and fibre column specimens, it is reasonable to assume that the lower curve represents the behaviour of confined con-

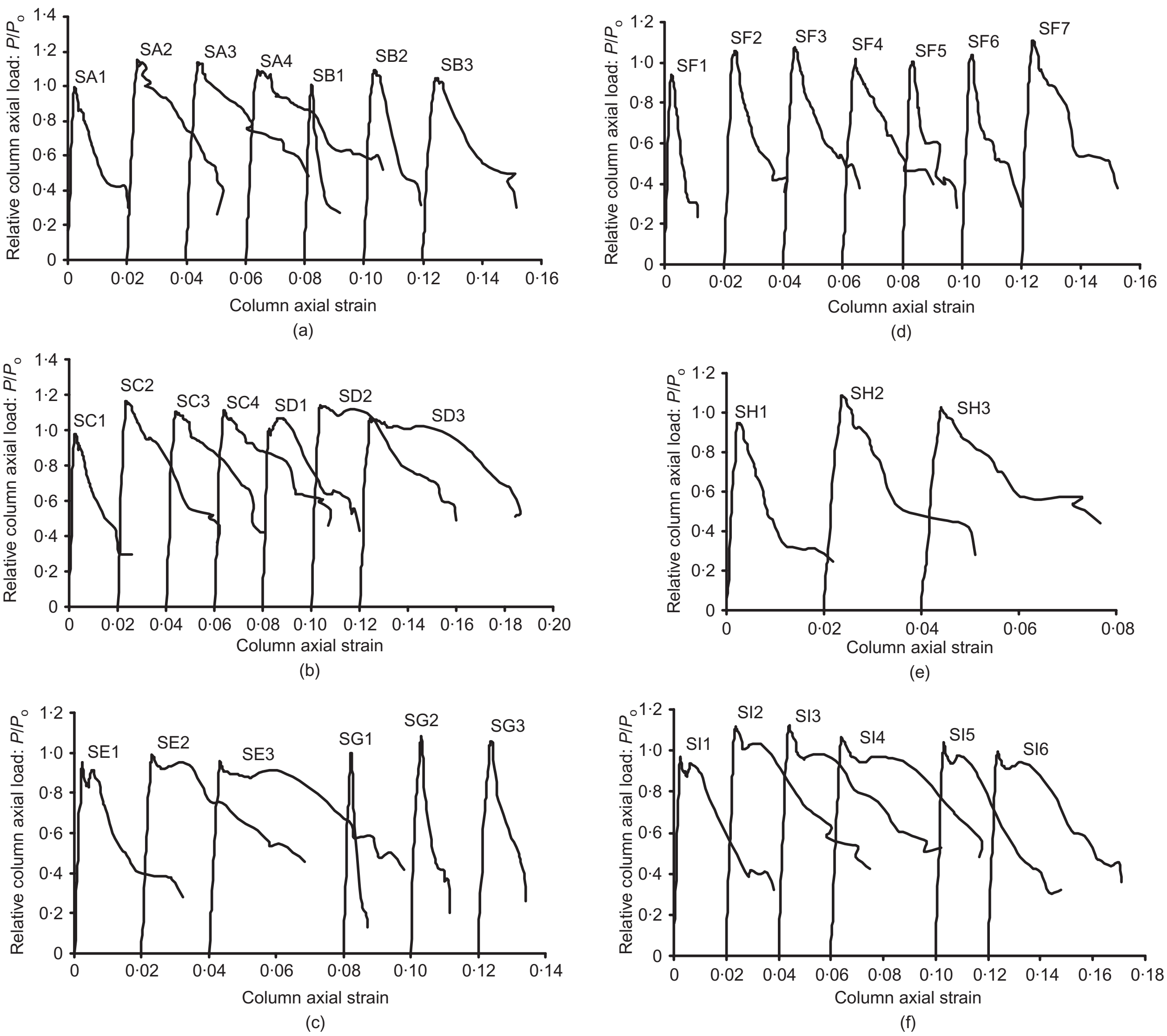

Fig. 4. (a)–(f) Total relative applied load plotted against axial strain curves for confined specimens

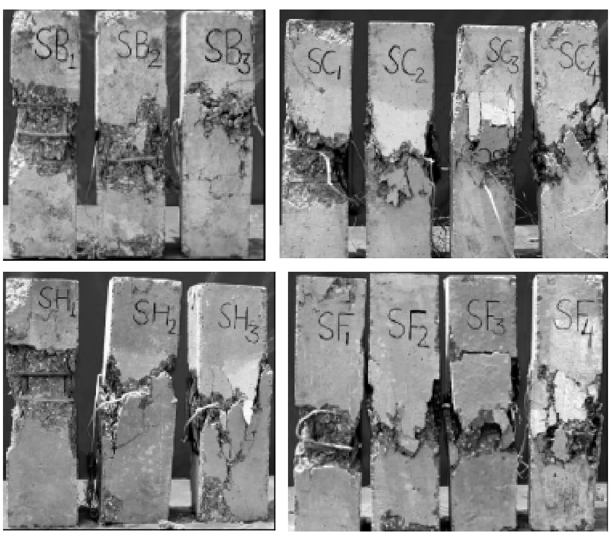

Fig 5. Appearance of some of the confined specimens after testing

crete up to the peak (point A). When the concrete cover becomes ineffective entirely, the response of confined concrete is given by the upper curve that follows point B, which was identified as corresponding to unconfined axial strains ε_{c50o} for both fibre and non-fibre concretes. Owing to the brittle failure of unconfined plain concrete specimens, their ε_{c50o} strain could not be measured accurately in the present study. In the absence of data, strain ε_{c50o} can be assumed to be equal to 0·004 for plain unconfined concrete.[17,18] However, the actual measured values of ε_{c50o} were used in establishing the point B in fibre-reinforced columns. In the region between point A and point B, cover can be considered to be partly effective. A smooth transition was assumed between points A and B.[17] Using this procedure, the behaviour of confined concrete was evaluated and peak-confined concrete load, P_{cc}, was computed for all the specimens. The maximum measured axial load P_{max} and computed loads P'_c (peak concrete load corre-

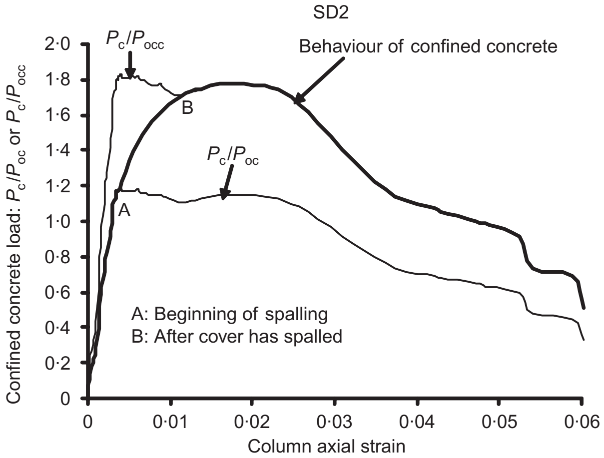

Fig 6. Confined concrete contribution curve

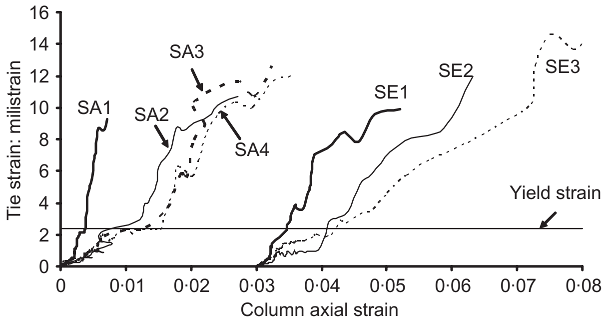

Fig 7. Variation of tie strains with column axial strains

sponding to the beginning of spalling) and P_{cc} (peak of confined concrete curve) for each specimen are given in Tables 3 and 4. These loads have been normalised with respect to the computed loads P_o, P_{oc} and P_{occ}, respectively, for comparison. For columns in which the peak of confined concrete curve was observed to be between points A and B, P_{cc} was computed from the load–strain curves after a smooth transition was introduced.

Strains in longitudinal and lateral steel

The strains in the longitudinal and lateral reinforcements were recorded by strain gauges as described earlier. To analyse these strains, the readings given by the two strain gauges attached to the longitudinal steel bars were averaged and, similarly, the readings of two strain gauges attached to the lateral steel were averaged. These average strains for both longitudinal and lateral steel corresponding to loads P'_c and P_{cc} are given in Tables 3 and 4. The notations ε'_l and ε'_h stand for average strains in longitudinal and lateral steel, respectively, at load P'_c and strains ε_{lcc} and ε_{hcc} denote average strain in longitudinal and transverse reinforcement, respectively at peak-confined load, P_{cc}. At peak load, P'_c, the longitudinal steel was found to have yielded but the strains in lateral confining steel were considerably less than their respective yield strains as indicated by the steel strain values shown in Tables 3 and 4. The lateral tie strains in fibre specimens were even less than the strains in non-fibre specimens. Fig 7 shows the variation of tie strains with axial column strains for a few specimens. It shows that the development of lateral strain is significantly diminished in the presence of fibres, indicating that the cracking is suppressed by the fibres. With the increase of applied axial strain, the tie strain in fibre columns gradually builds up as the fibres start pulling out of the matrix during the post-peak response and it even exceeds the transverse steel strains in non-fibre columns at higher axial strain values, indicating a more cohesive concrete with better bond between steel and tie bars.

Strength and ductility of confined specimens

The ratio P_{max}/P_o ranges from 0·93 to 1·07 for confined non-fibre specimens with an average value of 0·985 and varies from 0·97 to 1·16 for confined fibre-reinforced specimens with a mean value of 1·08. This suggests that the fibres helped to realise the theoretical columns' capacity, P_o, by preventing the premature cover spalling and even resulted in increased axial strengths compared with corresponding non-fibre column specimens. In all the fibre specimens (except SE2 and SE3) the applied maximum load, P_{max}, was found to be larger than P_o. The reason for the slightly lower axial strength of SE2 and SE3 specimens may be the closer spacing of lateral ties (30 mm) which, in addition to causing a separation between the core and the cover, prevented the fibres from properly reaching into the cover concrete and consequently allowed the cover to separate from the core earlier than expected. In fibre-reinforced concrete specimens, the ratio P_{max}/P_o increased with the increase in the fibre volume fraction at a constant aspect ratio, whereas it decreased slightly at the constant volume fraction, when the aspect ratio increased from 100% short fibres to 100% long fibres, for a given lateral confinement and concrete strength. The ratios P'_c/P_{oc} and $\varepsilon'/\varepsilon_{co}$ for non-fibre specimens indicate that their cover failed prematurely. However, these ratios for fibre-reinforced specimens confirm the delay in cover spalling owing to the incorporation of fibres into the HSC mix.

The ratio of peak-confined concrete loads P_{cc} (corresponding to second peak) to the unconfined theoretical load P_{occ} ranges from 1·10 to 1·68 (average value = 1·33) and from 1·12 to 1·77 (average value = 1·39) for non-fibre and fibre-reinforced specimens, respectively. Slightly higher ratios of P_{cc}/P_{occ} for fibre-reinforced column specimens indicate a nominal gain in confined strength owing to fibre addition. In the case of both fibre and non-fibre specimens, higher ratios were noticed for specimens with a higher degree of confinement and with lower concrete strength. However, in fibre-reinforced specimens, for a given lateral steel confinement and concrete strength, the load ratio P_{cc}/P_{occ} increased with an increase in the amount of fibres of any aspect ratio. For specimens having the same confinement, concrete strength and fibre content, the ratio P_{cc}/P_{occ} slightly decreased with an increase in the aspect ratio of fibres from 100% short fibres to 100% long fibres.

The strain corresponding to peak-confined load, ε_{cc}, and the post peak strains ε_{c85c} (axial strain at which the load drops to 85% of the peak-confined load) and ε_{c50c} (axial strain at which the load drops to 50% of the peak-confined load) were computed for all the specimens as reported in Tables 3 and 4. To characterise the deformability of confined concrete, these strain values were then normalised with respect to the unconfined plain concrete strain, ε_{co}. The area under the stress–strain curve, A_{cuc}, for confined concrete was also compared with the corresponding area, A_{cuo}, for unconfined plain concrete for all the column specimens (Tables 3 and 4). This area ratio is an indication of the toughness of confined concrete. In the case of non-fibre specimens, the strain ratios $\varepsilon_{cc}/\varepsilon_{co}$, $\varepsilon_{c85c}/\varepsilon_{co}$ and $\varepsilon_{c50c}/\varepsilon_{co}$ ranged from 1·08 to 3·01, from 1·35 to 5·91 and from 1·61 to 13·50, respectively and area ratio, A_{cuc}/A_{cuo} ranged from 1·52 to 12·17. The ratios $\varepsilon_{cc}/\varepsilon_{co}$, $\varepsilon_{c85c}/\varepsilon_{co}$ and $\varepsilon_{c50c}/\varepsilon_{co}$ varied from 1·44 to 9·91, from 1·69 to 18·14 and from 3·42 to 26·79 for fibre-reinforced specimens, while the toughness ratio A_{cuc}/A_{cuo} ranged from 3·25 to 23·55. It can be observed that these strain ratios and area ratios, which signify the deformability of HSC columns, are several times larger for fibre-reinforced concrete specimens than for non-fibre column specimens. This shows that the ductility of HSC column specimens increases considerably with the introduction of fibres in concrete.

Effect of test variables

Using the analysis procedure described previously, the final confined concrete contribution curves were established for all the specimens and used to evaluate the effects of different test variables on confined concrete behaviour. Fig. 8 shows the effect of volume fraction (v_f) of fibres on stress–strain behaviour of confined fibre-reinforced HSC. The test curves indicate that an increase in volume fraction of fibres results in a consistent increase in peak-confined strength (P_{cc}), corresponding peak strain (ε_{cc}), post-peak strains (ε_{c85c} and ε_{c50c}) and toughness (A_{cuc}). However, it was noticed that the gain in peak and post-peak strains and toughness were considerably more pronounced than those in peak strength. A maximum increase of 12% in the strength gain (P_{cc}/P_{oc}) and 219% in the toughness ratio (A_{cuc}/A_{cuo}) were observed as the fibre content increased from 0% in specimen SF1 to 2·0% in specimen SF7. A further analysis of the experimental data shows that the relative beneficial effect of fibre addition on the deformation capacity reduced as the amount of confinement increased. For example, if the pair of

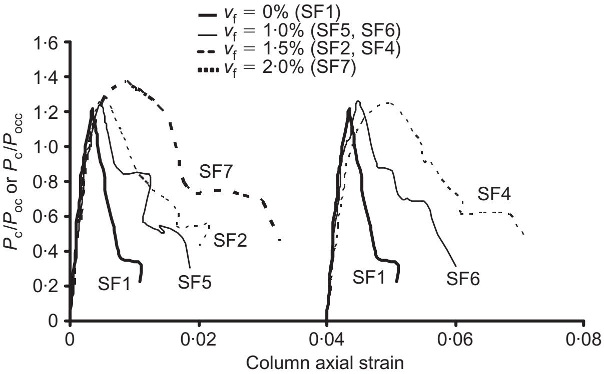

Fig 8. Effect of volume fraction (v_f) of fibres

specimens SG2–SG1 (single tie configuration and 2·2% volume ratio of ties) is compared with SI2–SI1 (double tie configuration and 5·62% of tie volume), the toughness ratio enhancement owing to fibres decreased from 114% to 73%, respectively. Similarly, the gain in toughness ratio decreased from 235% in the SB1–SB2 column pair having 2·2% volume ratio of ties to 119% in the SA1–SA2 column pair having 3·3% lateral steel content. Similar trends were noticed in most of the other comparable specimens.

The significance of fibre aspect ratio is illustrated in Fig. 9. It can be seen that as the aspect ratio of fibres increased from 20 (short fibres only) to 40 (long fibres only), the post-peak deformability of HSC increased. This may be attributed to the fact that under the increasing loads, once the cracks become quite wide in the post-peak region, the short fibres begin to pull out of the matrix and their crack bridging capability is relatively diminished as compared to longer fibres. The longer fibres can, however, arrest the propagation of these macro-cracks for a longer period of time and their gradual pull-out mode improves the post-peak ductility. It was, however, observed that the gain in peak-confined load (P_{cc}/P_{oc}) relative to non-fibre specimens was smaller in the case of specimens having only long fibres as compared with the column specimen with only short fibres for any given degree of confinement and concrete strength. This is probably attributable to

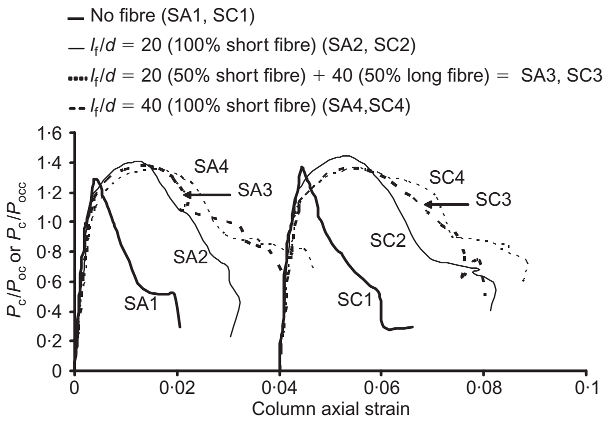

Fig 9. Effect of aspect ratio (l_f/d) of fibres

the fact that the short fibres are able to control better the initiation and propagation of initial micro-cracks. Short fibres therefore have a larger influence on the early part of matrix cracking, thereby enhancing the strength of the column, whereas longer fibres play their role to improve the post-peak toughness.

The stress–strain curves of specimens SA3, SC3, SF3 and SI3 exhibit the significance of the mixed aspect ratio of fibres. A perusal of test results and the stress–strain curves (for 100% short fibres, for 50% short fibres + 50% long fibres, for 100% long fibres), for a given parameter of confinement and concrete strength, indicates that at a given total fibre content, as the amount of short fibres increases, the peak stress increases, and the gain in toughness ratio decreases, whereas as the share of longer fibres increases the relative gain in post-peak toughness increases with a decrease in peak stress. This indicates that the combined use of short and long fibres created a better energy dissipation mechanism, the short fibres contributing at the early stage of cracking when the cracks were small in nature and the longer fibres effectively bridging the wider cracks at the later stage. Therefore, the mixed aspect ratio of fibres appears to be a good proposition for columns and it is postulated that advantages can be optimised in both peak-confined strength and ductility by judiciously mixing short and long fibres at some optimum proportions.

The effect of varying the degree of confinement on the behaviour of fibre-reinforced concrete specimens was observed to be similar to that on non-fibre concrete column specimens: strength and ductility improved with an increase in the amount and yield strength of lateral steel and better configuration of ties. Fig. 10 demonstrates the effect of the volumetric ratio and spacing of the confining reinforcement on confined non-fibre and fibre-reinforced HSC. (The responses of only three pairs of specimens are shown.) As expected, the larger the volumetric ratio or closer the spacing of lateral steel, the more ductile is the behaviour. The column specimens with reduced volumetric ratio or increased spacing of lateral steel exhibit a brittle behaviour, showing a faster rate of strength decay after the peak. A gain of 26% in confined strength (P_{cc}/P_{occ}), 236% enhancement in strain ductility ($\varepsilon_{c50c}/\varepsilon_{co}$) and 435% increase in the toughness ratio (A_{cuc}/A_{cuo}) were observed for non-fibre concrete specimens owing to an increase in the volumetric ratio of lateral ties from 2·2% in specimen SG1 to 5·5% in specimen SE1. The corresponding enhancements were 25% and 24% in confined strength, 320% and 292% in strain ductility and 422% and 385% in toughness ratio for fibre-reinforced concrete specimen pairs SG2–SE2 and SG3–SE3, respectively.

The significance of varying the yield strength of lateral ties is shown in Fig. 11, where different pairs of specimens have been compared. The compared specimens of each pair had the same concrete strength as well as the same volumetric ratio, arrangement and spacing of lateral steel and similar fibre properties (for fibre-reinforced columns) but different yield strengths. In the case of non-fibre specimens, the maximum enhancements of 7% (SF1–SH1) in the confined concrete strength ratio (P_{cc}/P_{occ}) and 60% (SF1–SH1) in the toughness ratio (A_{cuc}/A_{cuo}) were observed as a result of increasing the tie yield strength from 412 MPa to 520 MPa. In fibre-reinforced HSC specimens, maximum increase of 9% in strength and 42% in toughness ratios were observed for the pair of square specimens, SF2 plotted against SH2.

In this study it was possible to observe the effect of varying the lateral steel configuration by comparing the behaviour of square column specimens SE1, SE2 and SE3 with SI1, SI2 and SI4 respectively (Fig. 12). The

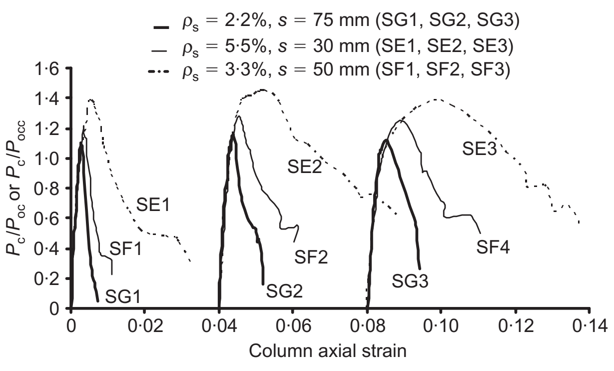

Fig 10. Effect of volumetric ratio and spacing of ties

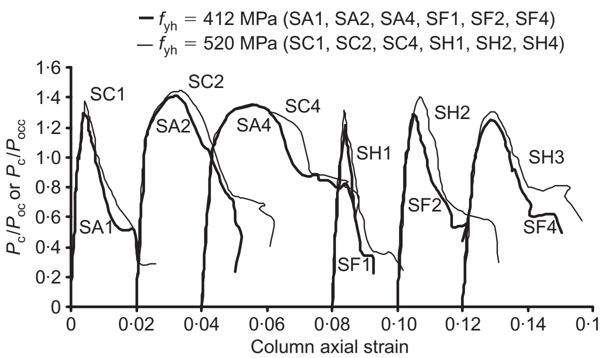

Fig 11. Effect of yield strength of ties

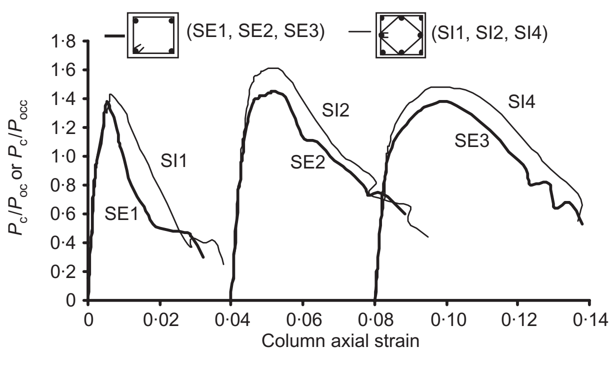

Fig 12. Effect of tie configuration and distribution of longitudinal steel

compared specimens had almost equal volumetric ratio of lateral steel and other parameters of confinement except the variable considered. The specimens SE1, SE2 and SE3 were constructed using single perimeter ties (4-bar arrangement), and SI1, SI2 and SI4 specimens had a double tie configuration (8-bar arrangement). An increase of 51% in the strain ductility ($\varepsilon_{c50c}/\varepsilon_{co}$) and 36% in the toughness ratio (A_{cuc}/A_{cuo}) were noticed in the SI1 specimen over the SE1 specimen. However, the ratio P_{cc}/P_{occ} is equal to 1·38 and 1·43 for specimens SE1 and SI1 respectively, showing a strength enhancement of only 3·5%. In the case of the fibre-reinforced HSC specimens, improvements of 10% and 6% in P_{cc}/P_{occ}, 15% and 9% in $\varepsilon_{c50c}/\varepsilon_{co}$ and 13% and 14% in A_{cuc}/A_{cuo} were seen as the transverse steel configuration was changed from the single-tie type in specimens SE2 and SE3 to the double-tie type in specimens SI2 and SI4, respectively.

The concrete compressive strength was one of the primary variables investigated extensively in the test programme. The behaviour of the specimens with the same volumetric ratio, spacing, configuration and yield strength of lateral steel, longitudinal steel ratio and properties of fibres (in the case of fibre-reinforced columns) but with different concrete strengths was compared to quantify the effects of this parameter. Fig. 13 shows a comparison of some of the specimens with different concrete strengths. The post-peak curves of the higher-strength concrete columns are somewhat steeper, indicating a faster rate of strength decay as compared with the lower HSC specimens. The results indicate reduced deformability and strength enhancement for both the non-fibre and fibre-reinforced concrete column specimens with increased concrete strength.

Summary and conclusions

This study reports the results of 96 tie-confined steel fibre-reinforced HSC short column specimens tested under concentric compression. The specimens were tested under monotonic concentric loading. Ideally the effects of flexure should be considered in addition to axial loads, but the complexity of analysis under combined axial load and flexure makes it difficult to study a large number of cases and monotonic concentric testing gives a reasonable assessment in the first instance. The effect of testing conditions such as frictional restraint between the loading platens and the specimen, the gauge length, the stiffness of the testing machine, the loading rate and the shape and the size of the specimen are also equally important; however, the same could not be considered in the present study. Within the scope of the present investigation, the following conclusions may be drawn.

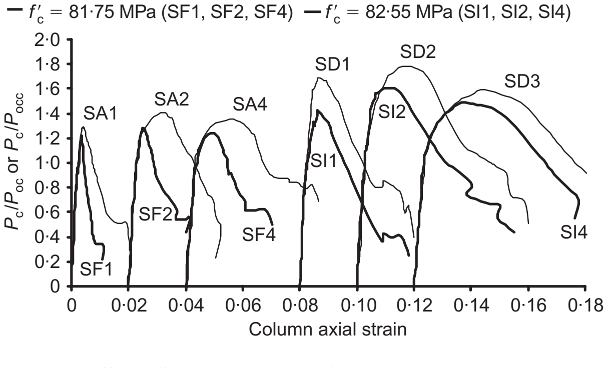

Fig 13. Effect of concrete strength

The strength and ductility of confined HSC increased with the addition of steel fibres in the concrete, the strength enhancement being less sensitive than ductility. The introduction of steel fibres prevented the early spalling of cover concrete in HSC column specimens. Unlike the specimens without fibres, almost all the confined specimens cast with fibre-reinforced concrete achieved peak loads higher than their respective theoretical strengths, indicating that the entire sectional area can be used in computing their load-carrying capacity.

The peak and post-peak strains in fibre-reinforced confined columns were several times larger than those in the comparable non-fibre columns. For a given tie confinement and concrete strength, the strength and ductility of confined concrete increased as the volume fraction of fibres increased. For constant fibre content, the toughness enhancement was higher for larger aspect ratio of fibres. The strength gain decreased slightly with the increase in the aspect ratio of fibres. The percentage improvements in column response are lower in columns containing larger amounts of tie steel. Therefore, the fibres can be more effectively utilised to enhance the performance of HSC columns if the lateral steel content is relatively low.

The results of specimens with a blend of short and long fibres (mixed aspect ratio) indicate that the improvements with respect to both strength and ductility can be optimised by judiciously mixing short and long fibres, which may not be provided by fibres of only one aspect ratio.

For the range of values considered in the present study, the effects of volumetric ratio, yield strength and configuration of ties on the behaviour of confined concrete appeared to be similar for both fibre and non-fibre concrete columns—that is, strength and ductility improved with the increase in these parameters. However, this study has quantified the effects of these key variables of confinement on steel fibre-reinforced concrete. Test data indicated that the tie confinement and fibres became less effective as the concrete strength increased. This further concludes that higher-strength concrete columns need either more fibre reinforcement for a given tie confinement or higher tie confinement for the same fibre content compared with lower concrete strength columns to achieve similar strength and ductility enhancements.

References

1. Li B., Park R. and Tanaka H. *Strength and Ductility of Reinforced Concrete Members and Frames Constructed Using High Strength Concrete*. University of Canterbury, Christchurch, New Zealand, 1994. Research report No. 94–5.
2. Cusson D. and Paultre P. High strength concrete columns confined by rectangular ties. *ASCE Journal of Structural Engineering*, 1994, **120**, No. 3, 783–804.
3. Razvi S. and Saaticioglu M. Strength and deformability of confined high strength concrete columns. *ACI Structural Journal*, 1994, **91**, No. 6, 678–687.
4. Bayrak O. and Sheikh S. A. Confinement reinforcement design considerations for ductile HSC columns. *ASCE Journal of Structural Engineering*, 1998, **124**, No. 9, 999–1010.
5. Sundraraja P. and Sheikh S. A. *High Strength Concrete Columns under Eccentric Loads*. Department of Civil Engineering, University of Toronto, Toronto, 1992, Research report.
6. Foster S. J. *Design and Detailing of High Strength Concrete Columns*. University of New South Wales, Sydney, Australia, 1999, Research report No. R-375.
7. Mansur M. A., Chin M. S. and Wee T. H. Stress–strain relationship of high strength fibre concrete in compression. *ASCE Journal of Materials in Civil Engineering*, 1999, **11**, No. 1, 21–29.
8. Campione G., Mindess S. and Zingone G. Compressive stress–strain behaviour of normal and high strength carbon fibre concrete reinforced with spirals. *ACI Materials Journal*, 1999, **96**, No. 1, 27–34.
9. Foster S. J. and Attard M. M. Strength and ductility of fibre-reinforced high strength concrete columns. *ASCE Journal of Structural Engineering*, 2001, **127**, No. 1, 281–289.
10. Hsu L. S and Hsu C. T. Stress–strain behaviour of steel fibre high strength concrete under compression. *ACI Structural Journal*, 1994, **91**, No. 4, 448–457.
11. Mangat P. S. and Azari M. M. Influence of steel fibre and stirrup reinforcement on the properties of concrete in compression members. *International Journal of Cement Composites and Lightweight Concrete*, 1985, **7**, No. 3, 183–192.
12. Ganesan N. and Murthy J. V. Strength and behaviour of confined steel fibre reinforced concrete columns. *ACI Materials Journal*, 1990, **87**, No. 3, 221–227.
13. Alsayed S. H. Confinement of reinforced concrete columns by rectangular ties and steel fibres. *Magazine of Concrete Research*, 1992, **44**, No. 161, 265–270.
14. Paultre P., Khayat K. H., Langlois Y., Trundel A. and Cusson D. Structural performance of some special concretes. *Proceedings of the 4th International Symposium on Utilization of High Strength/High Performance Concrete, Paris,* 1996, 787–796.
15. Collins M. P., Mitchell D. and MacGregor J. G. Structural design considerations for high strength concrete. *Concrete International*, 1993, **15**, No. 5, 27–34.
16. Foster S. J., Liu J. and Sheikh S. A. Cover spalling in HSC columns loaded in concentric compression. *ASCE Journal of Structural Engineering*, 1998, **124**, No. 12, 1431–1437.
17. Sheikh S. A. and Uzumeri S. M. Strength and ductility of tied concrete columns. *Journal of the Structural Division, ASCE*, **106**, No. 5, 1079–1102.
18. Cusson D. and Paultre P. Stress–strain model for confined high strength concrete. *ASCE Journal of Structural Engineering*, 1995, **121**, No. 3, 468–477.

Discussion contributions on this paper should reach the editor by 1 June 2008